

Original Article

Binding sensitivity of adefovir to the polymerase from different genotypes of HBV: molecular modeling, docking and dynamics simulation studies

Jing LI¹, Yun DU¹, Xian LIU¹, Qian-cheng SHEN¹, Ai-long HUANG^{2,*}, Ming-yue ZHENG^{1,*}, Xiao-min LUO¹, Hua-liang JIANG¹

¹Drug Discovery and Design Center, State Key Laboratory of Drug Research, Shanghai Institute of Materia Medica, Chinese Academy of Sciences, Shanghai 201203, China; ²Institute for Viral Hepatitis, Key Laboratory of Molecular Biology on Infectious Diseases, Ministry of Education, Chongqing Medical University, Chongqing 400016, China

Aim: To investigate the molecular mechanisms underlying the influence of DNA polymerase from different genotypes of hepatitis B virus (HBV) on the binding affinity of adefovir (ADV).

Methods: Computational approaches, including homology modeling, docking, MD simulation and MM/PBSA free energy analyses were used.

Results: Sequence analyses revealed that residue 238 near the binding pocket was not only a polymorphic site but also a genotype-specific site (His238 in genotype B; Asn238 in genotype C). The calculated binding free-energy supported the hypothesis that the polymerase from HBV genotype C was more sensitive to ADV than that from genotype B. By using MD simulation trajectory analysis, binding free energy decomposition and alanine scanning, some energy variation in the residues around the binding pocket was observed. Both the alanine mutations at residues 236 and 238 led to an increase of the energy difference between genotypes C and B ($\Delta\Delta G_{C-B}$), suggesting that these residues contributed to the genotype-associated antiviral variability with regard to the interaction with ADV.

Conclusion: The results support the hypothesis that the HBV genotype C polymerase is more sensitive to ADV than that from genotype B. Moreover, residue N236 and the polymorphic site 238 play important roles in contributing to the higher sensitivity of genotype C over B in the interaction with ADV.

Keywords: hepatitis; HBV; polymerase; genotype; adefovir; molecular dynamics simulation; free energy calculation

Acta Pharmacologica Sinica (2013) 34: 319–328; doi: 10.1038/aps.2012.146; published online 3 Dec 2012

Introduction

Hepatitis B virus (HBV) is a disease of global concern. This virus has infected approximately 400 million people worldwide, including 93 million people in China^[1,2]. HBV is a highly variable virus with mutations that occur because of a shortage of proofreading activity of the DNA polymerase, which results in the formation of different genotypes and subtypes^[3]. There are eight hepatitis B virus genotypes (A-H) throughout world. Genotypes B and C are the most common genotypes in Asia^[4]. Compared to genotype B, genotype C is associated with later HBeAg seroconversion, more severe liver disease and a higher incidence of hepatocellular carcinoma (HCC)^[5-7].

Currently, the available antiviral drugs include interferon-alpha (IFN- α) and nucleotide analogue inhibitors of HBV polymerase, among which lamivudine (3TC), telbivudine (LdT), entecavir (ETV), adefovir (ADV) and tenofovir (TDV) have been approved by the FDA^[8,9] (Figure 1). ADV is an acyclic nucleotide analog that inhibits the HBV DNA polymerase and suppresses HBV replication at the level of DNA synthesis. It is efficacious even for the treatment of lamivudine-resistant chronic hepatitis B^[10,11].

To treat patients with chronic hepatitis B, a personalized approach allows for the treatment efficacy to be optimized, which involves individualizing the therapy according to the genetic differences of the infectious agents. Recently, increasing evidence has shown that there are differences in the antiviral response among HBV genotypes^[12-16]. IFN- α therapy was reported to be less effective in European patients infected with genotype D compared to those infected with genotype A, whereas in the Asian population, genotype C showed

* To whom correspondence should be addressed.

E-mail ahuang1964@163.com (Ai-long HUANG);

myzheng@mail.shnc.ac.cn (Ming-yue ZHENG)

Received 2012-04-24 Accepted 2012-09-24

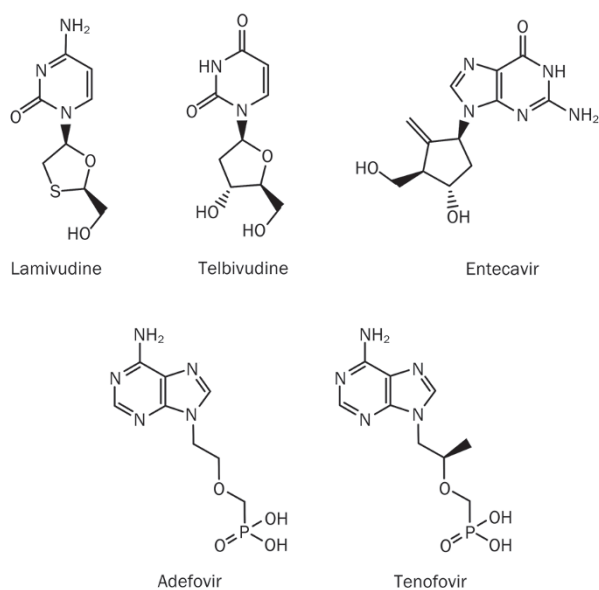


Figure 1. Chemical structures of five nucleotide analogue HBV polymerase inhibitor approved by US-FDA for treatment of HBV infection.

worse performance than genotype B. A clinical trial of 3TC has demonstrated that patients infected with HBV genotype A had higher DNA levels than those infected with genotype D^[17]. For ADV therapy, the data associated with the sensitivity among HBV genotypes are subtle, particularly between the two predominant genotypes in Asia, *ie*, B and C. Zeng *et al* identified a genotype-specific outcome, indicating that the HBV genotype B shows a greater reduction of viral DNA than genotype C (3.6 *vs* 3.1 logarithm copies/mL) at 48 weeks ADV post-treatment in a Chinese Han population with chronic HBV^[18]. However, another study of ADV therapy reported that a difference in the level of viral DNA reduction (3.42 *vs* 3.65 logarithm copies/mL) was observed after 48 weeks of treatment, although the association with HBV genotypes was not statistically significant^[19]. The differences in the average reduction of viral DNA could partially reflect the difficulty in analyzing the antiviral response to ADV therapy because the different ethnicities, endpoint definitions, sample size and whether the patients have been treated with other therapies would all affect the results of the clinical trials^[20].

Recently, a computational study of the possible mechanisms of the different inhibitory effects of benzothiadiazine molecules on HCV genotype-1a and genotype-1b NS5b polymerase was reported, in which the ligand sensitivity was investigated with homology modeling and molecular docking^[21]. Clearly, the structural information of the HBV polymerase from genotypes B and C would also be helpful for investigating the molecular basis of ADV sensitivity. Because the crystal structure of the HBV polymerase is not available, homology models based on the X-ray structure of HIV-1 RT have been reported and utilized for determining the molecular mechanism of inhibition and drug resistance^[8, 22–25]. Thus, no computational study was reported regarding the molecular basis of drug effi-

cacy among different HBV genotypes. In this study, the differences between genotypes B and C that influence the binding affinity of ADV are studied using computational approaches. Two 3D models were first constructed for the HBV polymerase from genotypes B and C. Molecular docking, dynamics simulations, and binding free-energy calculations were then performed to explore the binding patterns of ADV and provide insights into the difference in the binding free-energy of genotypes B and C.

Materials and methods

Representative sequence selection for different genotypes of HBV polymerase

HBV genotype classification is based on a nucleotide sequence divergence of 8%^[4], although in sequences of the same genotype, naturally occurring polymorphic sites are often observed. Therefore, consensus genotype reference sequences of HBV polymerase for genotypes B and C are essential for homology model construction. Using the NCBI virus sequence genotyping tool^[26, 27], standard reference sequences of genotypes B and C were obtained. The resulting sequences were then analyzed using the online alignment tool, ClustalW2^[28], to determine the representative sequences for the two genotypes.

Homology modeling of HBV polymerase-DNA complex

The genotype consensus reference sequences reported by Rhee *et al*^[9] were used to represent the HBV polymerase genotypes B and C. The sequence alignment between the two genotypes was performed using the EMBOSS online program^[29]. Many HIV-1 RT crystal structures are available in the PDB database. Because the complexed ligand, TDV, is a methyl derivative of ADV, the complexed structure of HIV-RT/TDV (PDB ID: 1T05) was selected as the template^[30]. The recently published alignment of HBV polymerase and HIV-1 RT that was developed by Daga *et al*^[25] was used as the reference template for modeling the HBV polymerase domain. Following the alignment, the homology models of genotypes B and C were built using the automated modeling module, MODELLER^[31], in the Discovery Studio (DS) software package version 3.0 (Accelrys, San Diego, CA, USA). The optimal level of the entire protein and loops was set to high and medium, respectively. The best structure for each genotype was then selected according to the PDF (probability density function) scores and the three-dimensional fit to the template protein. After the initial model was prepared, the coordinates of the template-primer DNA duplex (11/7), two Mg²⁺ cations and one original ligand [tenofovir diphosphate (TDV-DP)] were transferred from the template structure, 1T05, to form a quaternary complex. After the energy minimization, the geometric quality of the modeled structures was evaluated by PROCHECK^[32]. The protein structures were visualized with the PyMOL molecular viewer^[33].

Molecular docking

The molecular docking study was performed with the Glide program (version 5.5)^[34]. It should be noted that ADV is a

prodrug, and we modeled its bioactive form, ADV diphosphate (ADV-DP), which is generated through stepwise phosphorylation after the oral administration of ADV. The 3D conformation of ADV-DP was constructed according to the coordinates of the ligand, TDV-DP, which was deposited in the template structure of HIV-RT, by deleting a methyl group.

After the ligand preparation, each modeled protein was prepared with the protein preparation wizard in Maestro^[34]. The molecular docking was performed using standard precision (SP) protocols with default parameters. The docking poses were ranked by their glide scores, and the best predicted conformation in each system was used for the subsequent molecular dynamics simulation and binding energy analysis.

Molecular dynamics

Classical molecular dynamics simulations of docked conformation-HBV polymerase complexes were performed using the AMBER 9.0 suite^[35]. To make a reliable comparison, the two systems were treated with the same procedures described below.

The electrostatic potential of ADV-DP was computed with Gaussian03 at the HF/6-31G* level^[36], then the charges were assigned using the RESP (restrained electrostatic potential) methodology^[37]. The charges and force field parameters for ADV-DP were generated by an antechamber^[38]. The polyphosphate parameters of ADV-DP in our system were identical to those developed by Meagher *et al*^[39]. The AMBER ff03 force field^[40] and the general AMBER force field (GAFF)^[41] were chosen to create the potential of the proteins and ADV-DP, respectively. The systems were then solvated in a truncated octahedral box of TIP3P water molecules 10 Å away from the protein^[42]. Counter-ions of Cl⁻ were then added to obtain the electrostatic neutrality of the systems.

Prior to the MD simulations, stepwise energy minimizations were utilized to relax the two systems by the sander program in AMBER 9.0. First, 3000 minimization of water molecules/ions steps were performed using a combination of steepest descent and conjugate gradient methods. The solute atoms were frozen with a constraint of 100 kcal mol⁻¹·Å⁻². The systems were then relaxed with a constraint of 10 kcal mol⁻¹·Å⁻² for an additional 3000 minimization steps. Next, the side chains of the proteins were minimized with an additional 2500 steps. Finally, the entire systems were minimized with 2000 steps without any constraints.

In the MD simulations, the Particle-Mesh Ewald (PME) method was utilized to address the long-range electrostatic interactions and a cutoff of 10 Å was applied^[43]. All chemical bonds involving hydrogen atoms were constrained using the SHAKE algorithm^[44], and the time step used for the MD simulations was 2 fs. The system was gradually heated from 0 to 300 K over 50 ps molecular dynamics in the NVT ensemble. Subsequently, a short dynamics of the entire system was performed at 300 K for a further 110 ps to equilibrate the solvent. Finally, 3.7 ns MD simulations were conducted with a periodic boundary condition in the NPT ensemble (300 K, 1 atm). The analyses of MD trajectories were performed with the Ptraj

module of AMBER 9.0.

MM-PBSA calculations

The binding free energy (ΔG_{bind}) of ADV-DP in the two systems was calculated using the MM-PBSA method^[45]. ΔG_{bind} was computed as follows:

$$\Delta G_{\text{bind}} = \Delta G_{\text{complex}} - (\Delta G_{\text{protein}} + \Delta G_{\text{ligand}}) \quad (1)$$

$$\Delta G_{\text{bind}} = \Delta E_{\text{gas}} + \Delta G_{\text{solv}} - T\Delta S \quad (2)$$

$$\Delta E_{\text{gas}} = \Delta E_{\text{int}} + \Delta E_{\text{ele}} + \Delta E_{\text{vdw}} \quad (3)$$

$$\Delta G_{\text{solv}} = \Delta G_{\text{PB}} + \Delta G_{\text{SA}} \quad (4)$$

ΔE_{gas} , the sum of the molecular mechanical energies, is composed of three parts: internal energy (ΔE_{int}), electrostatic potential (ΔE_{ele}) and van der Waals potential (ΔE_{vdw}). The solvation free energy (ΔG_{solv}) can be divided into contributions from the polar solvation free energy (ΔG_{PB}) and the nonpolar (ΔG_{SA}). In the PB calculation, the solvent and solute dielectric constant values were set to 80 and 2, respectively. The LCPO method^[46] was used to estimate the non-polar contribution as follows: $\Delta G_{\text{SA}} = 0.0072 \cdot \Delta S_{\text{ASA}}$, where a probe radius of 1.4 Å was set for the SASA (solvent-accessible surface area) calculation^[35]. Because of the high computational demand for large molecules, such as proteins, and the rough estimate of the entropic contribution ($-T\Delta S$)^[47, 48] and because we are comparing the relative binding affinities of two similar systems (*ie*, HBV polymerase genotypes B and C complexed with the same inhibitor, ADV-DP), the entropic contribution of both systems is disregarded in this study. The energy difference between the two systems ($\Delta\Delta G_{\text{C-B}}$) is as follows:

$$\Delta\Delta G_{\text{C-B}} = \Delta G_{\text{bind, C}} - \Delta G_{\text{bind, B}} \quad (5)$$

This equation was used to measure the sensitivity of genotype C over B with regard to the interaction with ADV.

In our work, 100 snapshots extracted from the last 800 ps simulation trajectories of each system were used to calculate the binding free energy of ADV-DP in the HBV polymerase-DNA-Mg complex.

Free energy decomposition and computational alanine scanning

The contribution of each residue in the HBV polymerase was then analyzed using the MM/GBSA decomposition procedure^[49, 50]. The ΔG_{GB} was calculated using the generalized Born (GB) model^[51], and the ΔG_{SA} was computed with the ICOSA method^[49]. All the energy components were calculated using the same 100 snapshots.

Next, the computational alanine scanning was performed for the two complexed systems. Single site alanine mutations at residues 236 and 238 in both genotypes B and C proteins were generated by deleting atoms and truncating the mutated residues at C γ and replacing them with a hydrogen atom^[52]. The binding free energies of the alanine mutants were calculated using the MM-PBSA approach described above. The same 100 snapshots obtained from the last 800 ps of the MD trajectory were used.

Results

Homology model of HBV polymerase

A total of six standard reference sequences of genotypes B and

C were retrieved using the National Center for Biotechnology Information (NCBI) genotyping tool (*Supplementary Information Table S1*). The sequence analyses of these reference sequences revealed that amino acid (AA) 238 located near the ligand binding pocket is different among the six consensus genotypic reference sequences (*ie*, Gln/His/Asn is located at position 238 in genotype B and Asn is located at position 238 in genotype C), and all the other polymorphic sites between the two genotypes were found distant from the binding pocket. Further statistical analyses of the published sequences reported in NCBI confirmed the significant difference at position 238 between genotypes B and C. As shown in Table 1, the occurrence rates of His and Asn at this position are 81% in genotype B and 86% in genotype C, respectively.

Based on the above analyses, the amino acid at position 238 was set to His for genotype B and Asn for C. The overall consensus reference genotype sequences used to construct

Table 1. Statistics of a few major amino acid types at position 238 for different HBV genotypes.

Genotype	Number of published sequences			
	Total	Asn	His	Other
B	645	86	525 (81%)	34
C	1532	1317 (86%)	104	111

the homology models of the HBV polymerase genotype B and genotype C share a high identity of 93.3% (*Supplementary Information Table S2*). The sequence alignment of the HBV polymerase with HIV-1 RT is shown in Figure 2. The final homology models of the HBV polymerase genotypes B and C are shown as ribbon diagrams in Figure 3. Similar to the HIV-1 RT, the modeled structures of the HBV polymerase also

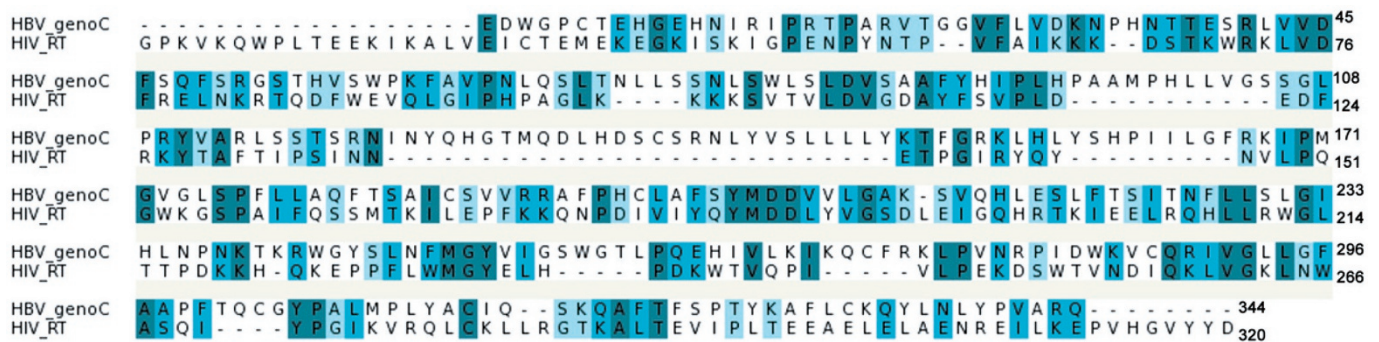


Figure 2. Alignment of HBV polymerase and HIV-1 RT sequences showing the identical (dark shaded) and closely related (light shaded) residues.

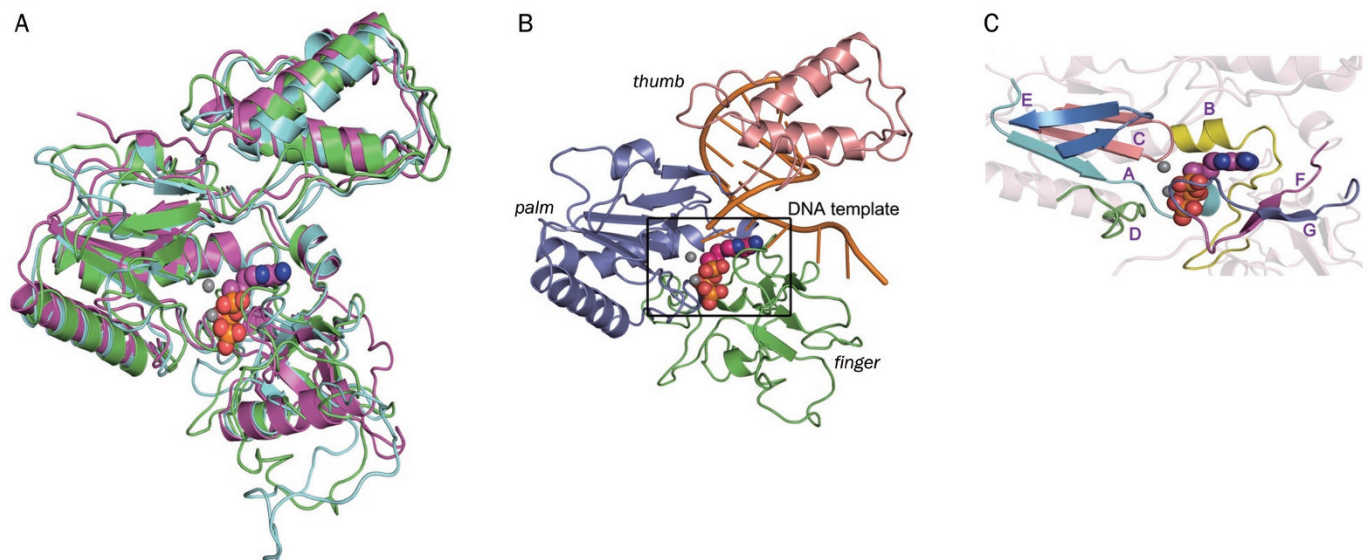


Figure 3. (A) Overall view of superposition of template structure 1T05 (magenta ribbon) with HBV polymerase genotype B (cyan) and C (green) model structures from homology modeling, ligand ADV-DP and two Mg^{2+} ions are highlighted in magenta and gray. (B) The 3D structural model of *finger*, *palm*, and *thumb* subdomains in HBV polymerase are represented in green, blue and salmon ribbons, respectively. DNA template-primer duplex is shown in orange cartoon mode. (C) The structurally conserved catalytic subdomains are displayed in colored ribbons: Domains A (cyan), B (yellow), C (pink), D (green), E (blue), F (magenta), and G (marine).

have three typical subdomains: *finger* (1 to 49 and 90 to 172), *palm* (50 to 89 and 173 to 267) and *thumb* (268 to 344)^[25] (Figure 3B).

As illustrated in Figure 3A, the two HBV polymerase models and HIV-1 RT structure resemble to each other in the *palm* and *thumb* regions; however, there is a major difference in the *finger* subdomain. The HBV polymerase has a larger *finger* region than the HIV RT and contains three long loops of 27, 11, and 9 residues in the HBV *finger* domain. Overall, the high similarity can be observed between the HIV-1 RT X-ray structure and the modeled HBV polymerase, particularly in the conserved catalytic subdomains, A-G^[53, 54], which are highlighted by different colors in Figure 3C. The structural variations of those two genotypes existed primarily in the flexible loop domain that is distant from ligand active site.

The homology models of the HBV polymerase genotypes B and C were then evaluated by PROCHECK^[32]. The overall G factors were -0.2 and -0.22 for genotypes B and C, respectively, indicating that the molecular geometries of the constructed models are stereochemically acceptable. The Ramachandran plots of the two models are shown in the supporting information (Supplementary Information Figure S1). Of all the residues, 81.7% and 82.2% are located in the most favored regions for genotypes B and C, respectively. Further analysis of the models revealed that all the disallowed residues except Met204 located in the YMDD motif were located distant from the putative ligand-binding site of the HBV polymerase. Consistent with Daga *et al*^[25], the corresponding Met residue was also found in the disallowed region of many HIV-1 RT crystal complexes, suggesting that the unusual configuration of Met204 is a valid and conserved feature. These evaluation results show that our homology models of HBV polymerase are of reasonable quality.

Docking studies of ADV diphosphate (ADV-DP) with HBV polymerase genotypes B and C

The superposition of the two docked complexes with the crystal protein, 1T05, suggests that the ADV-DP was docked into the active site with favorable poses, both bearing a close resemblance to the pose of the analogous ligand, TDV-DP, in 1T05. The best possible binding modes of ADV-DP in the HBV polymerase active sites of genotypes B and C are illustrated in Figure 4. Both complexes are stabilized by extensive hydrogen bonding networks. The nitrogen base of ADV-DP displayed two hydrogen bonds with the complementary base pair, dTMP, in the template chain. Moreover, it formed a π - π stacking interaction with the DNA base in the primer chain. The β -phosphate and γ -phosphate of the ligand formed a hydrogen bond with the backbone amide NH of Ala86 and Ala87. The side chains of Arg41 and Lys32 were involved in ionic interactions with the phosphate group of ADV-DP. Arg41, in the systems of genotypes B and C, formed three and two hydrogen bonds with ADV-DP, respectively. The carbonyl groups of Asp83, Asp205 and Val84 together with the three phosphate groups of ADV-DP formed a metal chelating interaction with the two Mg²⁺ ions that were present in the

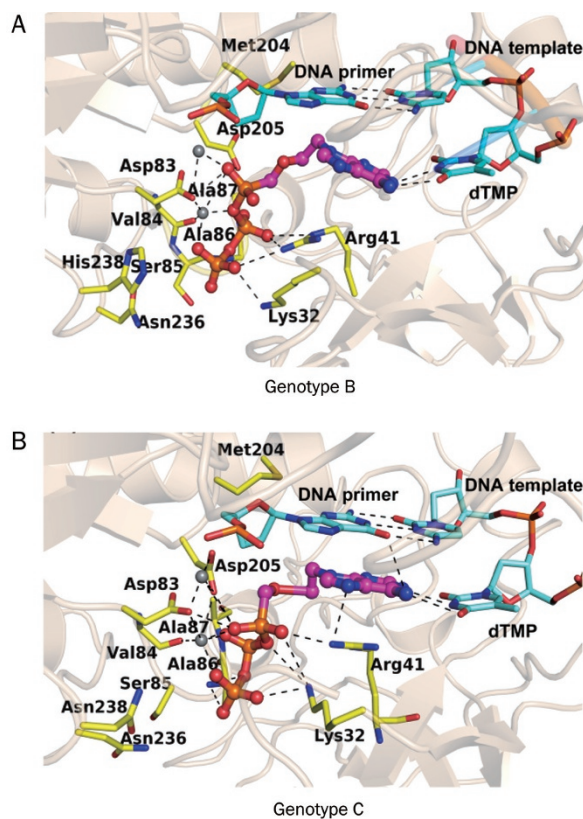


Figure 4. Binding modes of: (A) HBV polymerase genotype B and (B) genotype C with ADV-DP. Two Mg²⁺ ions are shown in gray colored spheres. The ligand ADV-DP is shown in magenta colored ball-and-stick mode. Mg²⁺ coordination and hydrogen bond interactions are shown with black dotted lines.

active site. The docking scores of the two genotypes, B and C, are also at the same level, with gscores of -10.25 and -10.07, respectively.

Assessing the binding mode of the different genotypes by MD simulation

To further validate our docked model, a molecular dynamics simulation was performed to obtain a more precise ligand-receptor state that is close to the natural behavior of the complex. The conformational stability of these two HBV polymerase-ADV complexes was assessed by performing a 3.8 ns molecular dynamics simulation in an explicit water model under the same conditions. The root mean square deviation (RMSD) values with respect to the initial structures were calculated along the 3.8 ns trajectories and are shown in Figure 5. The backbone RMSD values of the two systems tend to be convergent after 2 ns of simulation, with fluctuations approximately 4.5 Å and 4 Å for the structures of genotypes B and C, respectively. The RMSD change of the conserved catalytic subdomains, which is highlighted in Figure 3, exhibits a similar tendency. Intuitively, the lower conserved subdomain RMSD values of genotype C may suggest that the complex of ADV-DP bound within the HBV polymerase genotype C is in

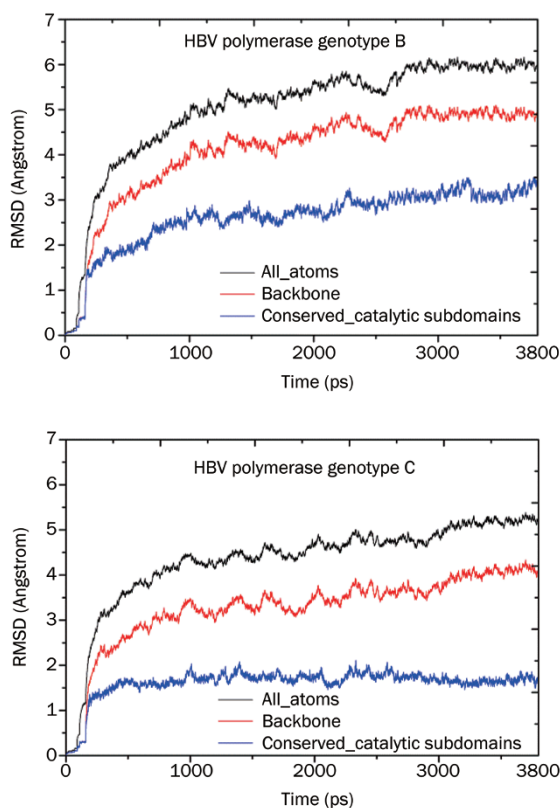


Figure 5. Root mean squared deviation (RMSD) of HBV polymerase homology model during the molecular dynamics simulation with respect to its starting (docked) pose.

a more stable state.

Figure 6 summarizes distance fluctuations of the corresponding atom pairs that are involved in the hydrogen bond interactions. As shown, some significant hydrogen bond interactions that were observed in the initial docking model (Figure 4) were maintained during the MD simulation. For example, two hydrogen bonds between the 6-amino purine ring of the ADV-DP and the paired base, dTMP, and the hydrogen bond between Arg41 and the α -phosphate of ADV-DP were maintained through the entire simulation of both systems. Moreover, we may also find a newly formed hydrogen bond between the γ -phosphate of ADV-DP and the hydroxyl group of Ser85 during the MD simulations.

The simulation system of genotype C showed superiority during the shorter time needed to form a steady hydrogen bonding interaction. Furthermore, the side-chain conformation of Ser85 in the genotype C system was further stabilized by a hydrogen bond with Asn236 in a loop region (Figure 6E), which was consistent with the binding pattern reported by Langley *et al*^[23]. However, in the genotype B system, the hydrogen bonding interaction between Ser85 and Asn236 was absent. The distance fluctuations that were observed from the MD simulations suggest that the different AA compositions at position 238 may affect the hydrogen bond formation between Ser85 and Asn236.

MM/PBSA free energy analyses

The binding free energies obtained from the MM/PBSA method are shown in Table 2. The table also lists the detailed contribution of the various energy components. It is clear from the table that the ADV-DP showed better binding affinity towards HBV polymerase genotype C than genotype B ($\Delta\Delta G_{C-B} = -20.96$ kcal/mol).

Table 2. MM-PBSA binding free energy estimations (kcal/mol) of HBV polymerase-DNA-Mg²⁺-ADV-DP complex of genotype B and C in the MD simulations.

Component ^a	Genotype B		Genotype C		$\Delta\Delta G_{C-B}$ ^d
	Mean ^b	Std ^c	Mean	Std	
ΔE_{ele}	-1393.11	32.60	-1215.80	33.19	177.31
ΔE_{vdW}	-26.27	6.26	-22.68	5.82	3.59
INT	0.02	0.04	0.03	0.03	0.01
ΔG_{SA}	-5.83	0.14	-6.06	0.11	-0.23
ΔG_{PB}	1298.34	28.47	1096.71	30.62	-201.63
ΔG_{PBSA}	1292.51	28.47	1090.64	30.62	-201.87
PBTOT	-126.85	8.60	-147.81	9.32	-20.96

^a Components: ΔE_{ele} , electrostatic energy; ΔE_{vdW} , van der Waals energy; INT, internal energy arising from bond, angle and dihedral terms in the MM force field; ΔG_{SA} , nonpolar contribution to the solvation free energy; ΔG_{PBSA} , solvation free energy, it is the sum of ΔG_{PB} and ΔG_{SA} ; PBTOT, final estimated binding free energy calculated from the terms above.

^b Average energy over 100 snapshots in the last 800 ps of MD simulation.

^c Standard error of mean values.

^d The energy difference between genotype B and C (C-B).

To provide quantitative information regarding the detailed contribution of the residues in the different HBV polymerase genotypes, free energy decomposition analysis was utilized to decompose the contributions to the binding energies on a per-residue basis. Many residues were found to exhibit influences on the binding to the inhibitor, ADV-DP. Several amino acid residues, Lys32, Arg41, Asp83, Ser85, Ala86, Ala87, Phe88, Asp205, and Asn236, and two DNA base pairs were validated to have significant positive contributions with an absolute energy greater than 1 kcal/mol. This is highlighted in Figure 7. Notably, ADV-DP binds to similar key residues in the two systems, which is consistent with the results of the docking study and MD simulation. The favorable contributions of Lys32, Arg41, Asp83, Ser85, Ala86, Ala87, and dTMP are due to the hydrogen bonding interactions with ADV-DP. The purine ring of ADV-DP formed a strong π - π stacking interaction with the primer DNA base, which also showed an obvious hydrophobic interaction with Phe88. Phe88 is located within the hydrophobic pocket comprised of Ala87, Phe88, Ile180, and Met204. This finding is consistent with the report by Daga *et al*^[25]. In addition, for most of the key residues, a slightly stronger binding energy contribution was found in the genotype C system.

As observed in Figure 7, positive contributions were made

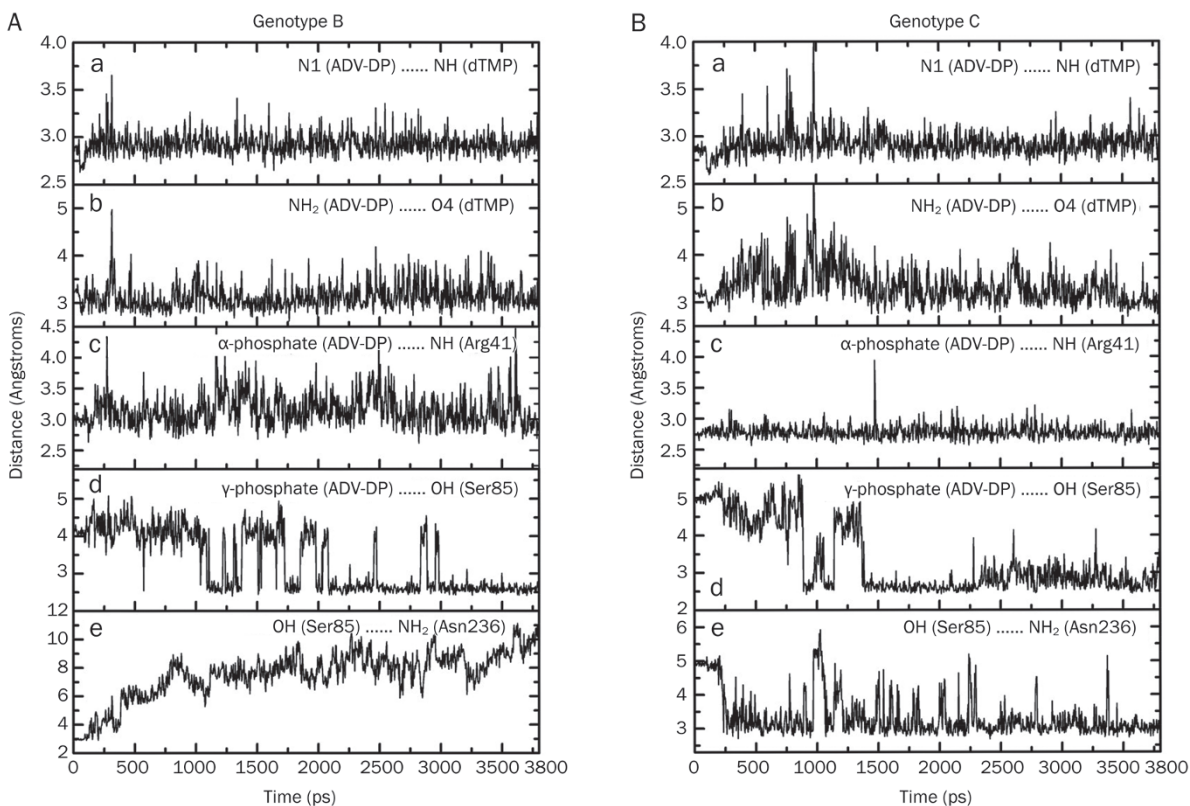


Figure 6. Distance graphs of some important hydrogen bonding interactions. Two maintained hydrogen bonds: (a) between N1 of ADV-DP and NH of dTMP; (b) and between NH₂ of ADV-DP and carbonyl O of dTMP. Panel (c) shows distance variations between α-phosphate of ADV-DP and the residue Arg41. (d) The residue Ser85 was distant in the beginning of the MD simulation; loop movement pushed the side chain amide toward the γ-phosphate of ADV-DP as described. (e) Distances between the hydroxyl group of Ser85 and NH₂ of Asn236. (A) Genotype B; (B) Genotype C.

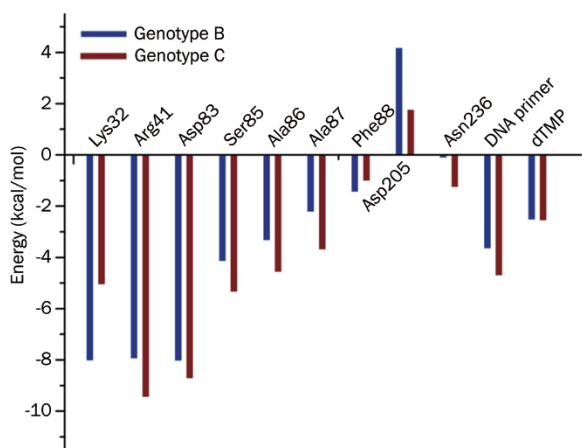


Figure 7. Decomposition of binding energy (GBTOT) on a per-residue basis, only residues making significant favorable or unfavorable contribution were shown ($|GBTOT| \geq 1.0$ kcal/mol).

for all the key residues except Asp205, which possibly arises from the repulsive interaction between the negatively charged side chain of Asp205 and the negatively charged phosphate group of ADV-DP. By contrast, the Mg²⁺ ions between Asp205

and the phosphate group of ADV in these two stable complexes (Figure 4) mediate a favorable coordination linkage between D205 and ADV-DP. The genotype-dependent, polymorphic residue 238 shows less contribution to the binding energy (≤ 1.0 kcal/mol). A lower residue contribution to genotype B than C was found at positions 236 and 238, which was verified by the computational alanine scanning results (shown in Table 3). Both the alanine mutations at residues 236 and 238 lead to losses of sensitivity, as reflected by an increase of the binding free energy difference between genotypes C and B ($\Delta\Delta G_{C-B}$). For the N236A mutant, the $\Delta\Delta G_{C-B}$ increased from -20.96 ($\Delta\Delta G_{C-B}$, wild type) to -18.66 kcal/mol ($\Delta\Delta G_{C-B}$, N236A). For

Table 3. Changes of MM-PBSA binding free-energy (kcal/mol) caused by the alanine mutations at the residue 236 and 238 in two genotypes systems.

	Genotype B	Genotype C	$\Delta\Delta G_{C-B}^*$
$\Delta G_{\text{bind, wild type}}$	-126.85	-147.81	-20.96
$\Delta G_{\text{bind, N236A}}$	-126.63	-145.29	-18.66
$\Delta G_{\text{bind, H/N238A}}$	-128.13	-148.09	-19.96

* The energy difference between genotype B and C (C-B).

the H/N238A mutant, the $\Delta\Delta G_{C-B}$ increased to -19.96 kcal/mol ($\Delta\Delta G_{C-B, H/N238A}$). These results confirmed our hypothesis that residues 236 and 238 contribute to the sensitivity of genotype C over B regarding the interaction with ADV-DP. Moreover, Asn236 is more important because the alanine mutation at this residue site causes a more significant loss of sensitivity.

Discussion

Hepatitis B is a growing problem worldwide. Genotypes B and C are the two predominant types of HBV in Asia. Clinical studies have been conducted to investigate the influence of specific genotypes on ADV treatment; however, the results are not yet conclusive. To further explore the underlying nature of the sensitivity of different genotypes of HBV polymerase to ADV, we used a computational protocol that combined homology modeling and binding free-energy calculations with MD simulations.

For the homology modeling of different genotypes of HBV polymerase, the representative sequence selection is of great significance. The statistical sequence analyses shown in Table 1 reveal that residue 238 near the binding pocket is not only a polymorphic site but is also a genotype-specific site (*ie*, His238 is present in genotype B and Asn238 is present in genotype C). This observation is consistent with previously reported sequence analysis results. An investigation of 192 treatment-naïve Chinese patients showed that position 238 is a genotype-dependent polymorphic site, in which 52/55 genotype B patients have a His at this position and 131/137 of genotype C patients have an Asn^[55]. Moreover, Rhee *et al* demonstrated that the AA types His238 and Asn238 are typical for B and C genotypes, respectively^[9].

In the polymerase/RT region, the sequence identity among various HBV strains is significant; however, the identity between HBV and other viruses is relatively low. HIV-1 RT shares approximately 25% sequence identity with HBV^[22] and has available crystal structures and is one of the nearest relatives of HBV polymerase. Many of the functionally important residues that are involved in the key protein-ligand interactions in HIV-1 RT are conserved between the HIV-1 RT structure and the HBV polymerase. These include the YMDD motif, the MGY motif and the catalytic triad of aspartic acid residues. For example, the catalytic triad Asp83, Asp205, and Asp206 of HBV polymerase correspond to Asp110, Asp185, and Asp186 in HIV RT (Figure 2). These three Asp residues are responsible for the coordination of two Mg²⁺ ions, which are very important for the activity of the polymerase. These data suggest that HIV-1 RT shares sufficient structural and functional similarity with HBV polymerase to serve as an excellent template to build a 3D structure for the HBV polymerase^[22-24]. In our work, the sequence alignment of our homology model referred to the alignment of the latest sequence published by Daga *et al*. Based on this sequence, the resulting homology model can match the results of the experimental mutation studies of the HBV polymerase^[25]. Only a minor modification was made at site Asn236 according to the work of Das *et al*^[22], in which Asn236 of the HBV polymerase

was aligned with Pro217 of HIV-RT instead of the Thr216 as in Daga's work. Asn236 is an important residue in the binding pocket of HBV polymerase and it is a primary drug resistance mutation site to ADV-DP^[56]. However, the alignment of Daga *et al* would result in the Asn236 in the constructed structure to be located too distant (~7 Å) from the nearest atom of the ligand (CTP), as suggested by their docking study. Therefore, for this residue, we chose the alignment of Das *et al* and used residue Pro217. As a result, the position of Asn236 in the constructed homology model is more feasible and is located in close vicinity to the binding site of ADV-DP. Apart from this, there are no other changes.

After the three-dimensional structure was successfully constructed, the ADV-DP was docked into the HBV polymerase-DNA complex. From the binding models, similar hydrogen-bond networks are observed for the ADV-DP in the HBV polymerase genotypes B and C. In addition, the gscores of the two systems are at the same level. All these indicate that the binding affinity that was predicted by docking could not discriminate between genotypes B and C. We must also note that molecular docking cannot fully account for the impact of protein flexibility, and a small change in receptor conformation may lead to a significant variation of binding affinity. Because identical structure templates were used in the homology modeling of the HBV polymerase genotypes B and C, the similar binding patterns of the two systems may simply be a result of the similar static protein conformations that were modeled. Therefore, to consider the flexibility of both the ligand, the protein and also their interactions with the surrounding water molecules, molecular dynamics simulations in combination with MM/PBSA free energy calculations were performed.

In summary, the calculated results support the hypothesis that the HBV polymerase genotype C is more sensitive to ADV than genotype B. Moreover, residue N236 and the polymorphic site 238 were further investigated and shown to play an important role in contributing to the sensitivity of genotype C over B in the interaction with ADV-DP. We believe that this work should provide a basis for the further investigation and understanding of the effect of polymerase genotypes on ADV treatment. This allows for the optimization of individual treatment and the minimization of side effects associated with HBV therapy.

Acknowledgements

This work is supported by the State Key Laboratory of Drug Research, Shanghai Institute of Materia Medica, Chinese Academy of Sciences. The authors gratefully acknowledge financial support from the State Key Program of Basic Research of China (No 2009CB918502), and the National Natural Science Foundation of China (No 81001399).

Author contribution

Ming-yue ZHENG and Ai-long HUANG designed the study, supervised the research and revised the manuscript. Jing LI performed the research, analyzed the data and wrote the manuscript. Yun DU, Xian LIU, Qian-cheng SHEN, Xiao-min LUO,

and Hua-liang JIANG discussed the results and commented on the manuscript.

Supplementary information

Supplementary Table and Figure are available at the Acta Pharmacologica Sinica website.

References

- Zoulim F, Parvaz P, Marcellin P, Zarski JP, Beaugrand M, Benhamou Y, et al. Adefovir dipivoxil is effective for the treatment of cirrhotic patients with lamivudine failure. *Liver Int* 2009; 29: 420–6.
- Li XD, Wang L, Zhong YW, Wong VW, Xu ZH, Liu Y, et al. Hepatitis B virus (HBV) subgenotypes C2 and B2 differ in lamivudine- and adefovir-resistance-associated mutational patterns in HBV-infected Chinese patients. *J Clin Microbiol* 2010; 48: 4363–9.
- Tanwar S, Dusheiko G. Is there any value to hepatitis B virus genotype analysis? *Curr Gastroenterol Rep* 2012; 14: 37–46.
- Ma Y, Ding Y, Juan F, Dou XG. Genotyping the hepatitis B virus with a fragment of the HBV DNA polymerase gene in Shenyang, China. *Virology* 2011; 8: 315.
- Chu CM, Liaw YF. Genotype C hepatitis B virus infection is associated with a higher risk of reactivation of hepatitis B and progression to cirrhosis than genotype B: a longitudinal study of hepatitis B e antigen-positive patients with normal aminotransferase levels at baseline. *J Hepatol* 2005; 43: 411–7.
- Yuen MF, Sablon E, Yuan HJ, Wong DK, Hui CK, Wong BC, et al. Significance of hepatitis B genotype in acute exacerbation, HBeAg seroconversion, cirrhosis-related complications, and hepatocellular carcinoma. *Hepatology* 2003; 37: 562–7.
- Yang HI, Yeh SH, Chen PJ, Iloeje UH, Jen CL, Su J, et al. Associations between hepatitis B virus genotype and mutants and the risk of hepatocellular carcinoma. *J Natl Cancer Inst* 2008; 100: 1134–43.
- Yadav V, Chu CK. Molecular mechanisms of adefovir sensitivity and resistance in HBV polymerase mutants: a molecular dynamics study. *Bioorg Med Chem Lett* 2004; 14: 4313–7.
- Rhee SY, Margeridon-Thermet S, Nguyen MH, Liu TF, Kagan RM, Beggel B, et al. Hepatitis B virus reverse transcriptase sequence variant database for sequence analysis and mutation discovery. *Antiviral Res* 2010; 88: 269–75.
- Sheng YJ, Liu JY, Tong SW, Hu HD, Zhang DZ, Hu P, et al. Lamivudine plus adefovir combination therapy versus entecavir monotherapy for lamivudine-resistant chronic hepatitis B: a systematic review and meta-analysis. *Virology* 2011; 8: 393.
- Angus P, Vaughan R, Xiong S, Yang H, Delaney W, Gibbs C, et al. Resistance to adefovir dipivoxil therapy associated with the selection of a novel mutation in the HBV polymerase. *Gastroenterology* 2003; 125: 292–7.
- Kao JH, Chen PJ, Lai MY, Chen DS. Hepatitis B genotypes correlate with clinical outcomes in patients with chronic hepatitis B. *Gastroenterology* 2000; 118: 554–9.
- Kao JH, Wu NH, Chen PJ, Lai MY, Chen DS. Hepatitis B genotypes and the response to interferon therapy. *J Hepatol* 2000; 33: 998–1002.
- Erhardt A, Reineke U, Blondin D, Gerlich WH, Adams O, Heintges T, et al. Mutations of the core promoter and response to interferon treatment in chronic replicative hepatitis B. *Hepatology* 2000; 31: 716–25.
- Kobayashi M, Arase Y, Ikeda K, Tsubota A, Suzuki Y, Saitoh S, et al. Clinical characteristics of patients infected with hepatitis B virus genotypes A, B, and C. *J Gastroenterol* 2002; 37: 35–9.
- Zollner B, Petersen J, Schafer P, Schroter M, Laufs R, Sterneck M, et al. Subtype-dependent response of hepatitis B virus during the early phase of lamivudine treatment. *Clin Infect Dis* 2002; 34: 1273–7.
- Cooksley WG. Do we need to determine viral genotype in treating chronic hepatitis B? *J Viral Hepat* 2010; 17: 601–10.
- Zeng AZ, Deng H, Yang C, Xin XJ, Li QL, Guo JJ, et al. Hepatitis B virus genotype-associated variability in antiviral response to adefovir dipivoxil therapy in Chinese Han population. *Tohoku J Exp Med* 2008; 216: 205–11.
- Westland C, Delaney W 4th, Yang H, Chen SS, Marcellin P, Hadziyannis S, et al. Hepatitis B virus genotypes and virologic response in 694 patients in phase III studies of adefovir dipivoxil. *Gastroenterology* 2003; 125: 107–16.
- Raimondi S, Maisonneuve P, Bruno S, Mondelli MU. Is response to antiviral treatment influenced by hepatitis B virus genotype? *J Hepatol* 2010; 52: 441–9.
- Wang X, Yang W, Xu X, Zhang H, Li Y, Wang Y. Studies of benzothiadiazine derivatives as hepatitis C virus NS5B polymerase inhibitors using 3D-QSAR, molecular docking and molecular dynamics. *Curr Med Chem* 2010; 17: 2788–803.
- Das K, Xiong X, Yang H, Westland CE, Gibbs CS, Sarafianos SG, et al. Molecular modeling and biochemical characterization reveal the mechanism of hepatitis B virus polymerase resistance to lamivudine (3TC) and emtricitabine (FTC). *J Virol* 2001; 75: 4771–9.
- Langley DR, Walsh AW, Baldick CJ, Eggers BJ, Rose RE, Levine SM, et al. Inhibition of hepatitis B virus polymerase by entecavir. *J Virol* 2007; 81: 3992–4001.
- Bartholomeusz A, Tehan BG, Chalmers DK. Comparisons of the HBV and HIV polymerase, and antiviral resistance mutations. *Antivir Ther* 2004; 9: 149–60.
- Daga PR, Duan J, Doerksen RJ. Computational model of hepatitis B virus DNA polymerase: molecular dynamics and docking to understand resistant mutations. *Protein Sci* 2010; 19: 796–807.
- <http://www.ncbi.nlm.nih.gov/projects/genotyping/view.cgi?db=2>.
- Rozanov M, Plikat U, Chappey C, Kochergin A, Tatusova T. A web-based genotyping resource for viral sequences. *Nucleic Acids Res* 2004; 32: W654–9.
- <http://www.ebi.ac.uk/Tools/msa/clustalw2/>.
- <http://www.ebi.ac.uk/Tools/psa/>.
- Tuske S, Sarafianos SG, Clark AD, Ding JP, Naeger LK, White KL, et al. Structures of HIV-1 RT-DNA complexes before and after incorporation of the anti-AIDS drug tenofovir. *Nat Struct Mol Biol* 2004; 11: 469–74.
- Sali A, Potterton L, Yuan F, van Vlijmen H, Karplus M. Evaluation of comparative protein modeling by MODELLER. *Proteins* 1995; 23: 318–26.
- Laskowski RA, MacArthur MW, Moss DS, Thornton JM. Procheck - a program to check the stereochemical quality of protein structures. *J Appl Crystallogr* 1993; 26: 283–91.
- <http://www.pymol.org>.
- Schrödinger Suite: Schrödinger, LLC, In. New York; 2008.
- Case DA, Cheatham TE 3rd, Darden T, Gohlke H, Luo R, Merz KM Jr, et al. The Amber biomolecular simulation programs. *J Comput Chem* 2005; 26: 1668–88.
- Frisch MJ, Trucks GW, Schlegel HB, Scuseria GE, Robb MA, Cheeseman JR, et al. Gaussian 03, Revision B.05 Gaussian, Inc, Wallingford, CT (2004).
- Bayly CI, Cieplak P, Cornell WD, Kollman PA. A well-behaved electrostatic potential based method using charge restraints for deriving atomic charges – the resp model. *J Phys Chem-U S* 1993; 97: 10269–80.
- Wang JM, Wang W, Kollman PA. Antechamber: an accessory software

- package for molecular mechanical calculations. *Abs Pap Am Chem Soc* 2001; 222: U403–U03.
- 39 Meagher KL, Redman LT, Carlson HA. Development of polyphosphate parameters for use with the AMBER force field. *J Comput Chem* 2003; 24: 1016–25.
- 40 Duan Y, Wu C, Chowdhury S, Lee MC, Xiong G, Zhang W, *et al*. A point-charge force field for molecular mechanics simulations of proteins based on condensed-phase quantum mechanical calculations. *J Comput Chem* 2003; 24: 1999–2012.
- 41 Wang J, Wolf RM, Caldwell JW, Kollman PA, Case DA. Development and testing of a general amber force field. *J Comput Chem* 2004; 25: 1157–74.
- 42 Jorgensen WL, Chandrasekhar J, Madura JD, Impey RW, Klein ML. Comparison of simple potential functions for simulating liquid water. *J Chem Phys* 1983; 79: 926–35.
- 43 Darden T, York D, Pedersen L. Particle mesh ewald – an N.Log(N) method for ewald sums in large systems. *J Chem Phys* 1993; 98: 10089–92.
- 44 Larini L, Mannella R, Leporini D. Langevin stabilization of molecular-dynamics simulations of polymers by means of quasisymplectic algorithms. *J Chem Phys* 2007; 126: 104101.
- 45 Kollman PA, Massova I, Reyes C, Kuhn B, Huo S, Chong L, *et al*. Calculating structures and free energies of complex molecules: combining molecular mechanics and continuum models. *Acc Chem Res* 2000; 33: 889–97.
- 46 Weiser J, Shenkin PS, Still WC. Approximate atomic surfaces from linear combinations of pairwise overlaps (LCPO). *J Comput Chem* 1999; 20: 217–30.
- 47 Yang B, Hamza A, Chen G, Wang Y, Zhan CG. Computational determination of binding structures and free energies of phosphodiesterase-2 with benzo[1,4]diazepin-2-one derivatives. *J Phys Chem B* 2010; 114: 16020–8.
- 48 Wan S, Coveney PV. Molecular dynamics simulation reveals structural and thermodynamic features of kinase activation by cancer mutations within the epidermal growth factor receptor. *J Comput Chem* 2011; 32: 2843–52.
- 49 Gohlke H, Kiel C, Case DA. Insights into protein-protein binding by binding free energy calculation and free energy decomposition for the Ras-Raf and Ras-RaIGDS complexes. *J Mol Biol* 2003; 330: 891–913.
- 50 Venken T, Krnavek D, Munch J, Kirchhoff F, Henklein P, De Maeyer M, *et al*. An optimized MM/PBSA virtual screening approach applied to an HIV-1 gp41 fusion peptide inhibitor. *Proteins* 2011; 79: 3221–35.
- 51 Onufriev A, Bashford D, Case DA. Exploring protein native states and large-scale conformational changes with a modified generalized born model. *Proteins* 2004; 55: 383–94.
- 52 Massova I, Kollman PA. Computational alanine scanning to probe protein-protein interactions: A novel approach to evaluate binding free energies. *J Am Chem Soc* 1999; 121: 8133–43.
- 53 Stuyver LJ, Locarnini SA, Lok A, Richman DD, Carman WF, Dienstag JL, *et al*. Nomenclature for antiviral-resistant human hepatitis B virus mutations in the polymerase region. *Hepatology* 2001; 33: 751–7.
- 54 Warner N, Locarnini S, Kuiper M, Bartholomeusz A, Ayres A, Yuen L, *et al*. The L80I substitution in the reverse transcriptase domain of the hepatitis B virus polymerase is associated with lamivudine resistance and enhanced viral replication *in vitro*. *Antimicrob Agents Chemother* 2007; 51: 2285–92.
- 55 Liu BM, Li T, Xu J, Li XG, Dong JP, Yan P, *et al*. Characterization of potential antiviral resistance mutations in hepatitis B virus reverse transcriptase sequences in treatment-naïve Chinese patients. *Antiviral Res* 2010; 85: 512–9.
- 56 Li XG, Liu BM, Xu J, Liu XE, Ding H, Li T. Discrepancy of potential antiviral resistance mutation profiles within the HBV reverse transcriptase between nucleos(t)ide analogue-untreated and -treated patients with chronic hepatitis B in a hospital in China. *J Med Virol* 2012; 84: 207–16.